LA-UR-12-22500
Approved for public release; distribution is unlimited.

Title: Density Functional Theory Calculations of Mass Transport in UO2

Author(s): Andersson, Anders D.
Dorado, Boris
Uberuaga, Blas P.
Stanek, Christopher R.

Intended for: ICDIM, 2012-06-24 (Santa Fe, New Mexico, United States)

Density functional theory calculations of mass transport in UO_2

In this talk we present results of density functional theory (DFT) calculations of U, O and fission gas diffusion in UO_2. These processes all impact nuclear fuel performance. For example, the formation and retention of fission gas bubbles induce fuel swelling, which leads to mechanical interaction with the clad thereby increasing the probability for clad breach. Alternatively, fission gas can be released from the fuel to the plenum, which increases the pressure on the clad walls and decreases the gap thermal conductivity. The evolution of fuel microstructure features is strongly coupled to diffusion of U vacancies. Since both U and fission gas transport rates vary strongly with the O stoichiometry, it is also important to understand O diffusion.

In order to better understand bulk Xe behavior in $UO_{2\pm x}$ we first calculate the relevant activation energies using DFT techniques. By analyzing a combination of Xe solution thermodynamics, migration barriers and the interaction of dissolved Xe atoms with U, we demonstrate that Xe diffusion predominantly occurs via a vacancy-mediated mechanism. Since Xe transport is closely related to diffusion of U vacancies, we have also studied the activation energy for this process. In order to explain the low value of 2.4 eV found for U migration from independent damage experiments (not thermal equilibrium) the presence of vacancy clusters must be included in the analysis.

Next we investigate species transport on the (111) UO_2 surface, which is motivated by the formation of small voids partially filled with fission gas atoms (bubbles) in UO_2 under irradiation. Surface diffusion could be the rate-limiting step for diffusion of such bubbles, which is an alternative mechanism for mass transport in these materials. As expected, the activation energy for surface diffusion is significantly lower than for bulk transport. These results are further discussed in terms of engineering-scale fission gas release models.

Finally, oxidation of UO_2 and the importance of cluster formation for understanding thermodynamic and kinetic properties of UO_{2+x} are investigated.

Density Functional Theory Calculations of Mass Transport in UO_2

David Andersson[1], Boris Dorado[2], Blas Uberuaga[1] and Chris Stanek[1]

[1]Los Alamos National Laboratory, Los Alamos, NM

[2]CEA, DEN, DEC, Centre de Cadarache, France

Funding acknowledgement: DOE Nuclear Energy Fuel Cycle Research and Development (FCRD) Campaign, Nuclear Energy Advanced Modeling and Simulation (NEAMS) Program.

Motivation and Objectives

- Formation, redistribution and release of FG are critical determinants of nuclear fuel performance.
- The first controlling step for FG release is diffusion of individual gas atoms to existing gas bubbles or grain boundaries (sinks) governed by the activation energy for bulk diffusion.
- For predictive capabilities need to establish underlying atomistic mechanisms and determine model parameters.
- The next step in the fission gas release process is interactions with microstructure features.

D.R. Olander, "Fundamental Aspects of Nuclear Reactor Fuel Elements" (1976)

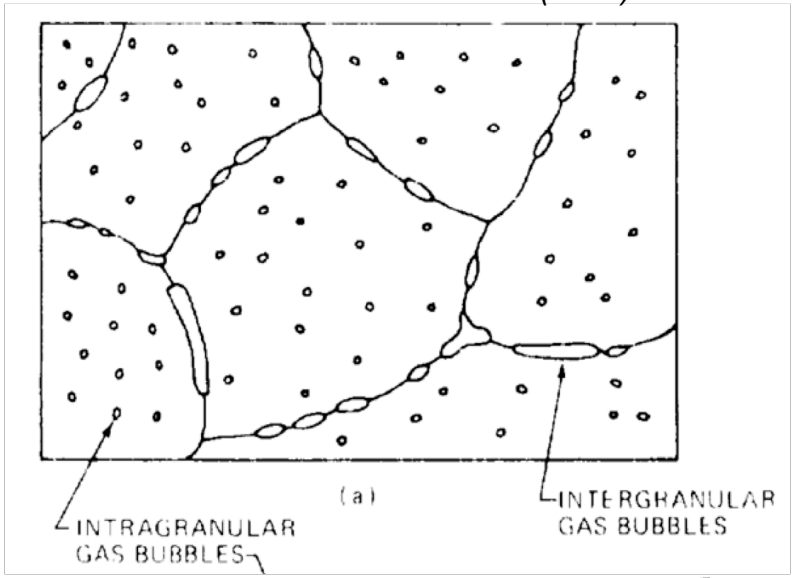

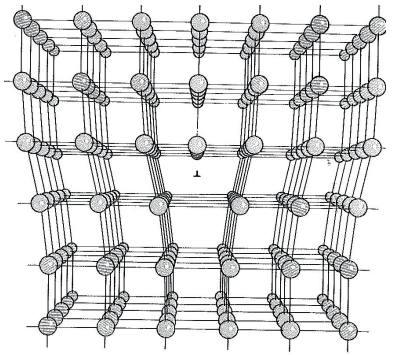

From C.A. Wert and R.M. Thomson "Physics of Solids" (1964).

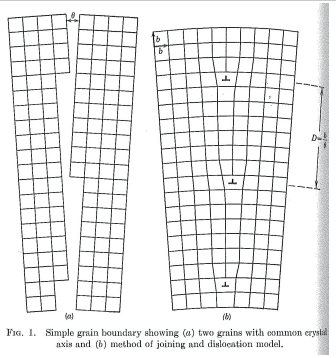

From W.T. Read Jr. and W. Shockley, in F. Seitz "Imperfections in Nearly Perfect Crystals" (1952).

Atomistic Simulations to Reveal Fission Gas Diffusion Mechanistics

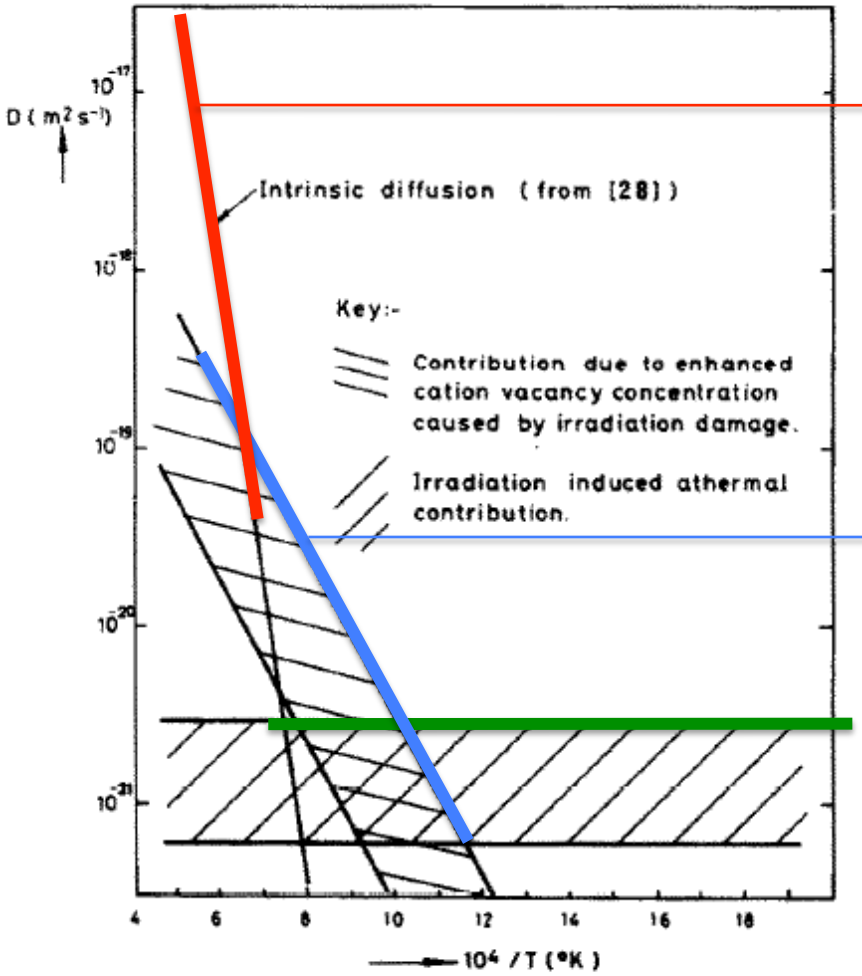

Fig. 10. Possible components of the in-pile rare gas diffusion coefficient.

Turnbull et al., J. Nucl. Mater. 107, 168 (1982).

Thermal diffusion $D = 7.6 \cdot 10^{-10} \exp\left(-\frac{3.04}{k_B T}\right)$

Calculations for the same conditions yield 3.94 eV, in good agreement with more recent measurements of intrinsic diffusion (3.9 eV).

Enhanced diffusion $D = C \times \sqrt{\dot{F}} \exp\left(-\frac{1.20}{k_B T}\right)$

Enhanced vacancy concentration due to irradiation. Improved data for unit processes yields 3.17 eV. Better agreement with FG bubble transport controlled by surface diffusion (1.00-1.25 eV).

Model was derived for stoichiometric UO_2, currently limited consideration of changes in stoichiometry, composition, etc.

Experimental Activation Energies for U and Xe Diffusion in $UO_{2\pm x}$

Experiments, e.g. Hj. Matzke, *Radiation Effects* **53** (1980) 219.

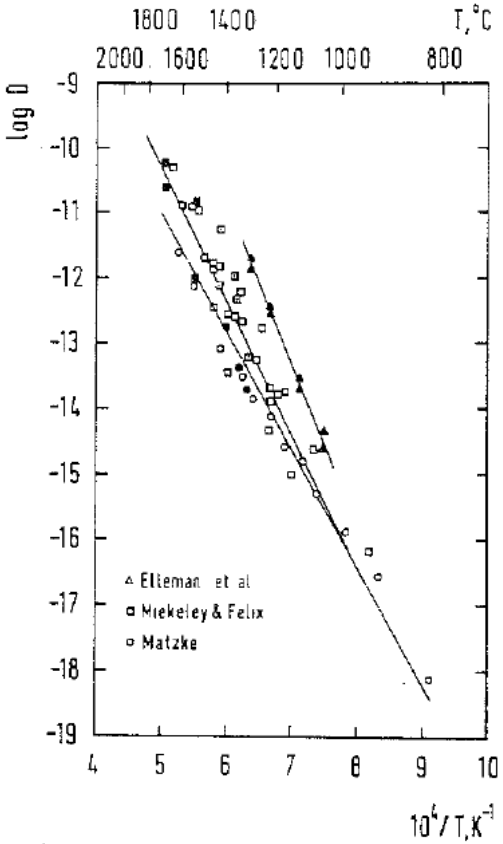

ΔH_A Xe:

ΔH_A=6.0 eV UO_{2-x}.

ΔH_A=3.9 eV UO_2.

ΔH_A=1.7 eV UO_{2+x}.

ΔH_A U:

ΔH_A=7.8 eV UO_{2-x}.

ΔH_A=5.6 eV UO_2.

ΔH_A=2.6 eV UO_{2+x}.

Easier to form U vacancy for x>0 and x=0 than for x<0.

- Effective activation energies determined decades ago, but mechanistic aspects not well understand.

$$D = D_0 \exp\left(-\frac{\Delta H_A}{k_B T}\right)$$

- Required for formulating accurate and predictive diffusion models that account for irradiation.

ED

Methodology

- Density functional theory calculations using VASP.
- Lichtenstein LDA+*U* for U 5f electrons. Literature values for *U* (*U*=4.5 and *J*=0.51 eV). AFM magnetic order is prescribed in all simulations.
- Electronic ground-state determined by occupation matrix control (Dorado *et al.*, PRB 82 035114 (2010), PRB 79 235125 (2009)), reduced symmetries, structural distortions and other methods (e.g., Meredig et al. PRB 82 195128 (2010) and Geng et al. Phys. Rev. B 82, 094106 (2010)).
- 2×2×2 and 2×2×3 fluorite supercell. Ionic relaxations, volume kept fixed.
- MD to find minimum energy structures for complex defects.
- Nudged elastic band (NEB) technique for calculation of migration barriers.
- Charged supercells to model mixed valence character.
- For details see Andersson et al., PRB 84 054105 (2011).

First Principles Calculations of Bulk Xe Diffusion

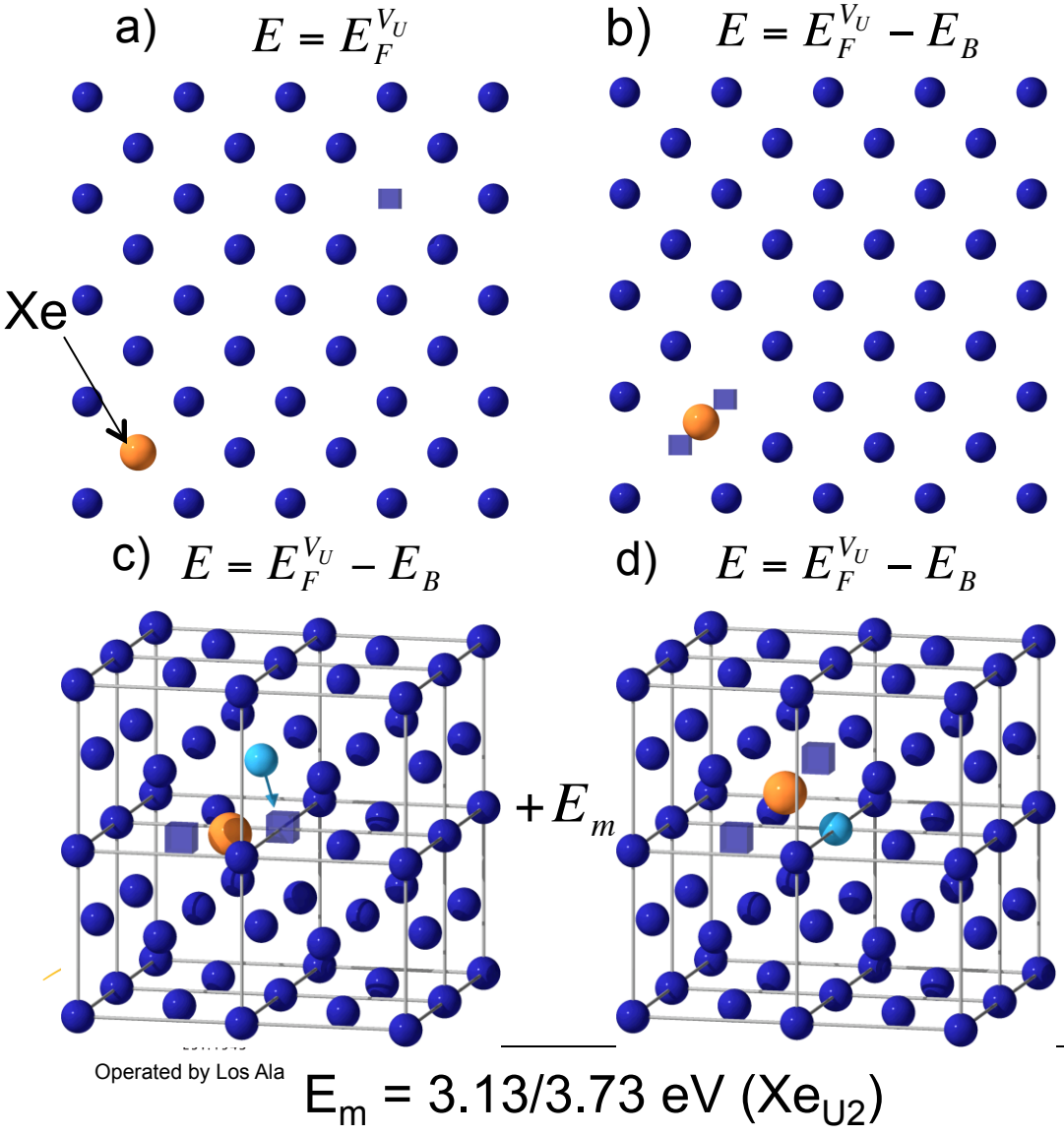

$$\Delta E_a^{Xe} = E_{VU}^{F} - E_B + E_m^{VU,C}(T)$$

Xe atoms occupy different trap sites as function of the $UO_{2\pm x}$ stoichiometry.

	$E_m^{VU,C}$ (eV)
Xe_{U2}	3.77
Xe_{U2O}	5.28
Xe_{U2O2}	5.13

Fluorite structure:

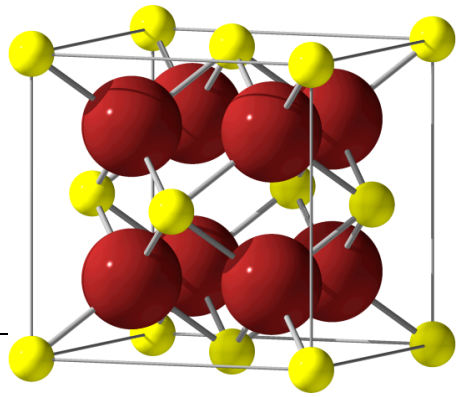

E_m = 3.13/3.73 eV (Xe_{U2})

Bulk U Diffusion Mechanism from DFT

$$\Delta E_a^U = E_{VUOx}^F + E_m^{VUOx}(T)$$

V_U
≈3.53-4.81 eV

V_{UO}
≈3.39-4.07 eV

V_{UO2}
≈3.76-4.51 eV

V_{U2}/V_{U2O}
1.69-2.61 eV/
2.17-2.92 eV

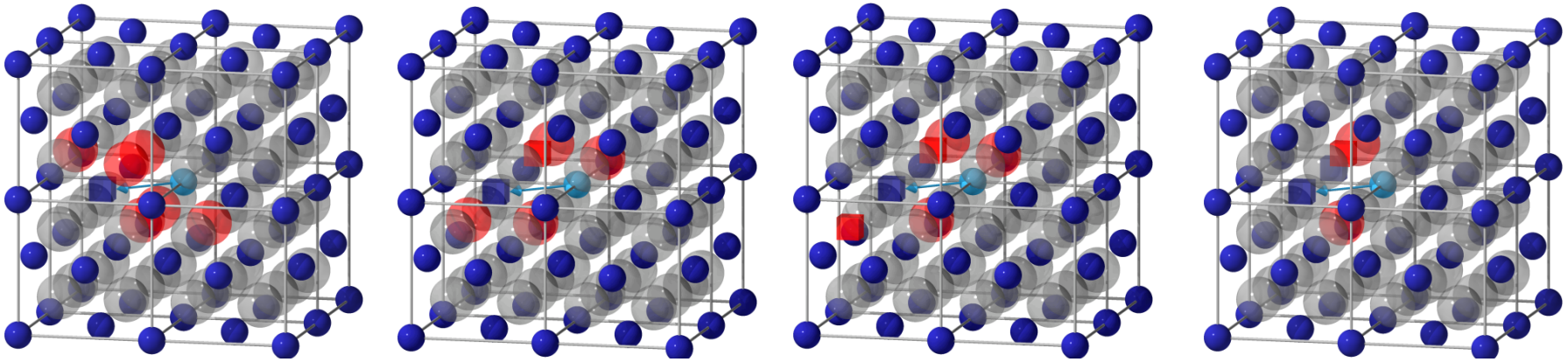

- High barrier is for a_0=5.45 (LDA+*U*) and low barrier for a_0=5.525 (GGA+*U*), possibly related to thermal expansion but current assessment put higher confidence in the LDA+*U* barrier.
- Significant displacement of neighboring O ions for V_U, V_{UO} and V_{UO2}.
- V_U different from exp. barrier (2.4 eV). Explained by V_{U20} or V_{U2} clustering. Experimental barrier obtained for damaged materials.

Calculating the Defect Parameters; Charge Compensation

$$E_a^{Xe} = E_{VU}^{F} - E_B + E_m^{VU,C}(T)$$

Simplified thermodynamic defect model due to Catlow[1]

	UO_{2-x}	UO_2	UO_{2+x}
V_U	$E_t=E_S$	$E_t=E_S-E_F$	$E_t=E_S-2E_F$
V_{UO}	$E_t=E_S-B_{dv}$	$E_t=E_S-\frac{1}{2}E_F-B_{dv}$	$E_t=E_S-E_F-B_{dv}$
V_{UO_2}	$E_t=E_S-B_{nt}$	$E_t=E_S-B_{nt}$	$E_t=E_S-B_{nt}$

Oxygen Frenkel pair as an example:

V_O+I_O

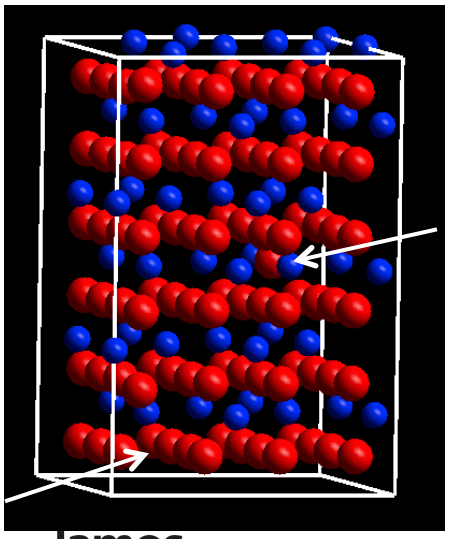

or

V_O + I_O

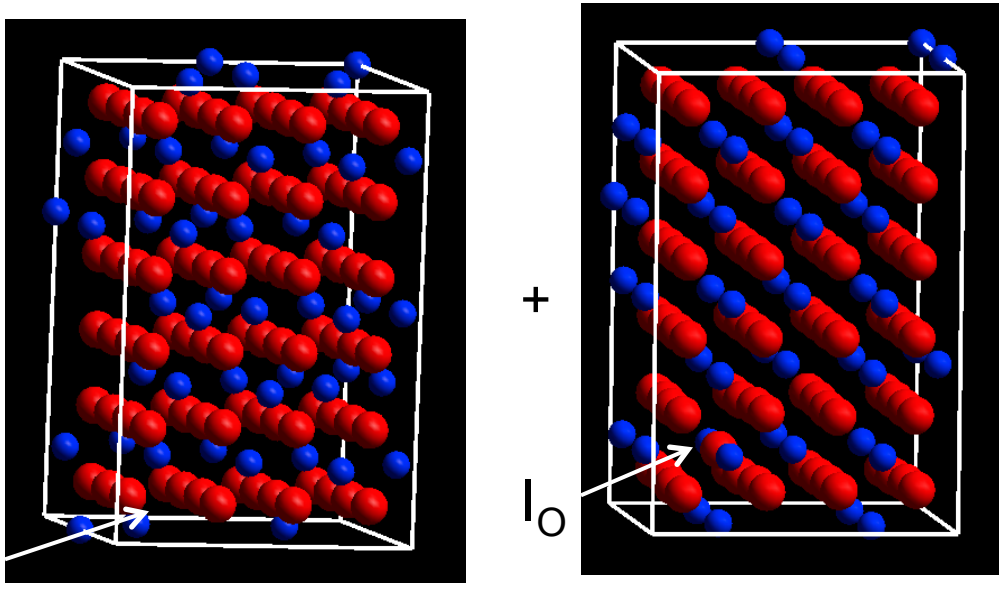

Listen to Crocombette (next talk) for extensive work on this topic.

First Principles Calculations of Defect Formation Energies

Simplified thermodynamic defect model due to Catlow[1]

	UO_{2-x}	UO_2	UO_{2+x}
V_U	$E_t=E_S$	$E_t=E_S-E_F$	$E_t=E_S-2E_F$
V_{UO}	$E_t=E_S-B_{dv}$	$E_t=E_S-\frac{1}{2}E_F-B_{dv}$	$E_t=E_S-E_F-B_{dv}$
V_{UO_2}	$E_t=E_S-B_{nt}$	$E_t=E_S-B_{nt}$	$E_t=E_S-B_{nt}$

$$\Delta E_a^{Xe} = E_{VU}^F - E_B + E_m^{VU,C}(T)$$

$$\Delta E_a^U = E_{VUOx}^F + E_m^{VUOx}(T)$$

	E_F (eV)	E_S (eV)	B_{dv}(eV)	B_{nt} (eV)
Neutral	5.26/6.40	10.15/11.96	2.93/3.35	5.58/6.46
Charged	3.32/4.26	6.00/7.65	1.22/1.52	1.43/3.15
One supercell	3.39/4.10	6.39/7.12	1.20/1.33	1.82/1.62
Ref. Exp[1,2]	3.0-4.0	6-7	--	--

"Fluorite"/"J-T"

- Charged supercell calculations include corrections for Coulomb interactions and potential alignments.

Charged or One supercell give best agreement with experiments.

[1] C. R. A. Catlow, Radiat. Eff. Defect. S. 53, 127 (1980).
[2] Hj. Matzke, in Diffusion Processes in Nuclear Materials, ed. R. P. Agarwala, North-Holland, Amsterdam, 1992.

Comparison of First Principles Results to Experimental Values

$$\Delta E_a^{Xe} = E_{VU}^F - E_B + E_m^{VU,C}(T)$$

$$\Delta E_a^U = E_{VUOx}^F + E_m^{VUOx}(T)$$

	Calc.	Exp[1]
$\Delta E_a^U(UO_{2-x})$	7.94-8.69	7.8
$\Delta E_a^U(UO_2)$	6.52-7.20	5.6
$\Delta E_a^U(UO_{2+x})$	2.90-4.18	2.6
$\Delta E_a^{Xe}(UO_{2-x})$	6.52-7.12	6.0
$\Delta E_a^{Xe}(UO_2)$	4.39-4.99	3.9
$\Delta E_a^{Xe}(UO_{2+x})$	1.47-2.07	1.7

[1] Hj. Matzke, in Diffusion Processes in Nuclear Materials, ed. R. P. Agarwala, North-Holland, Amsterdam, 1992.

	Calc.	Exp. [1]
$E_B(Xe_{UO2})$	2.69 (2.32-3.49)	--
$E_B(Xe_{UO})$	1.43 (1.30-1.95)	--
$E_B(Xe_U)$	1.02 (0.36-1.48)	--
$E_M(V_U)$	3.53-4.81	2.4*
$E_M(V_{UO})$	3.39-4.07	
$E_M(V_{UO2})$	3.76-4.51	--
$E_M(V_{U2})$	1.69-2.61	--
$E_M(V_{U2O})$	2.17-2.92	--
$E_M(Xe_{U2})$	3.77	--
$E_M(Xe_{U2O})$	5.28	--
$E_M(Xe_{U2O2})$	5.13	--

*"Incorrect" assignment.

Improved Modeling of U and Xe Diffusion

Collaboration with CEA Cadarache:

First-principles calculations of uranium diffusion in uranium dioxide

Boris Dorado,[1,2] David A. Andersson,[1,*] Christopher R. Stanek,[1] Marjorie Bertolus,[2]
Blas P. Uberuaga,[1] Guillaume Martin,[2] Michel Freyss,[2] and Philippe Garcia[2]

[1] *Materials Science and Technology Division, Los Alamos National Laboratory, Los Alamos, New Mexico 87545, USA*
[2] *CEA, DEN, DEC, Centre de Cadarache, 13108 Saint-Paul-lez-Durance, France*

- Previous model assumed that experiments were performed at fixed stoichiometry ($UO_{2\pm x}$). Incorrect assumption.
- First-principles DFT calculations combined with new thermodynamic model for defect chemistry were used to assess U self-diffusion in nearly stoichiometric UO_2.

$$E_a^{V_U} = 2E_{O_I} + E_S - 2E_{eh} - 2E_{FP_O} + E_{p_{O2}} + E_m^{V_U}$$

Updated thermochemical model and $E_m^{VU,C}$

	Calc.	Exp[1]
$\Delta E_a^{U}(UO_{2-x})$	7.64	7.8
$\Delta E_a^{U}(UO_2)$	3.97	5.6/4.4
$\Delta E_a^{U}(UO_{2+x})$	3.19	2.6
$\Delta E_a^{Xe}(UO_{2-x})$	5.61	6.0
$\Delta E_a^{Xe}(UO_2)$	3.94	3.9
$\Delta E_a^{Xe}(UO_{2+x})$	1.79	1.7

- Most favorable mechanism: O-assisted vacancy mechanism with activation energy 4.1-4.9 eV (experimental value: 4.4 eV).
- Interstitial diffusion gives higher E_a. The U interstitial(cy) migration barrier is 3.7 eV.

Interstitial Xe Diffusion in UO_2

Interstitial diffusion mechanism relevant if thermal or radiation-induced defects (i.e. vacancies) are present only in low concentrations.

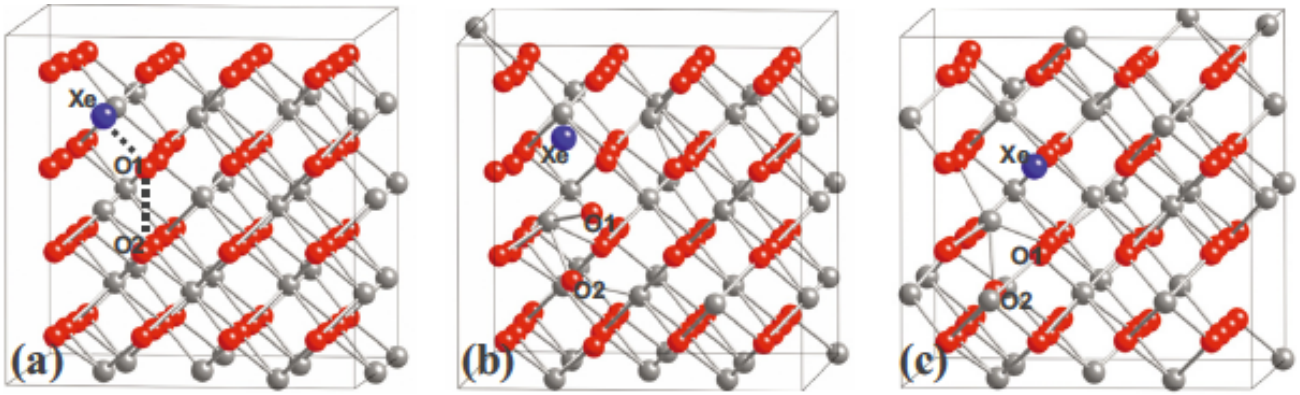

$E_M(Xe_I)$ A	4.48–5.29
$E_M(Xe_I)$ B	1.6-2.41

Liu et al (*APL*, **98** (2011) 151902)

ΔQ from fuel performance models:

	ΔQ [eV]		ΔQ [eV]
Q1 F&M [2007]	3.09	Q2 F&M Frapcon	1.97
Q2 F&M [2007]	1.19	Q3 F&M Frapcon	0.82
Q1 F&M Frapcon	0.57	ANS5.4	3.14

First Principles Analysis of Intermediate T Mechanisms

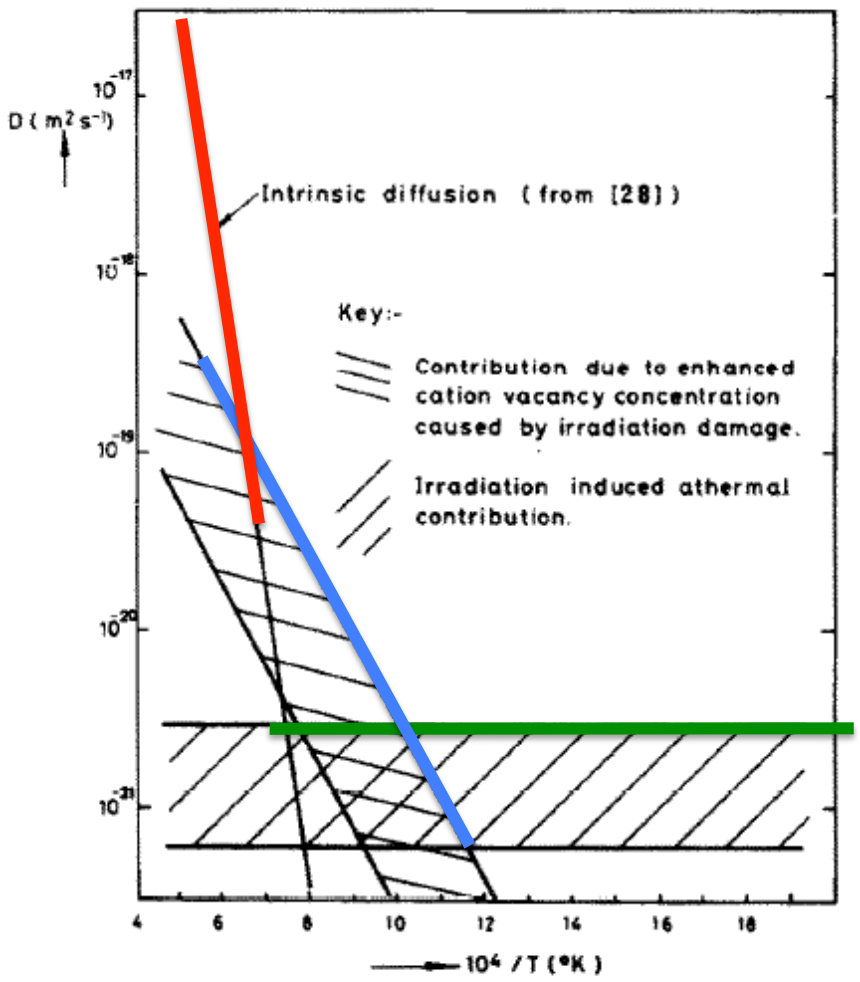

Fig. 10. Possible compon coefficient.

Traditionally explained by enhanced vacancy concentration according to:

$$D_2 = s^2 J_V V \qquad V \approx V_{irr} = \sqrt{K'/J_V Z}$$

$$D_2 = \text{constant} \times \sqrt{\dot{F}} \exp\left(\frac{-1.2}{k_B T}\right)$$

Obtained by assuming: $J_V \propto \exp\left(-\frac{2.4}{k_B T}\right)$

$$J_{Xe} \propto \exp\left(-\frac{E_m^{Xe_{U_2O}} - E_B^{Xe_{U_2O}}}{k_B T}\right)$$

From DFT:

$$J_V \propto \exp\left(-\frac{E_m^{V_{U_2}}}{k_B T}\right)$$

Applying the same assumption as above yields yields 3.17 eV. Interestingly this is close to the high temperature regime.

Further analysis required, alternative mechanisms may be important for intermediate T and high T.

Bubble Migration Controlled by Surface Diffusion

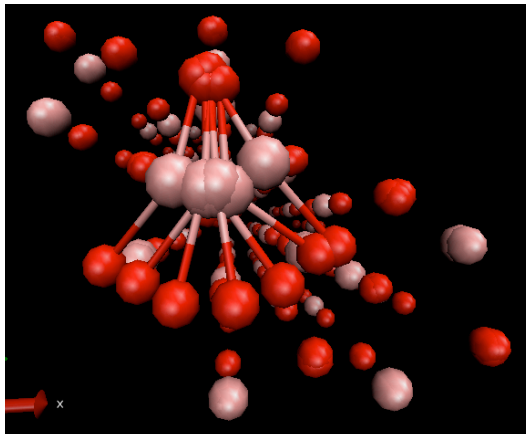

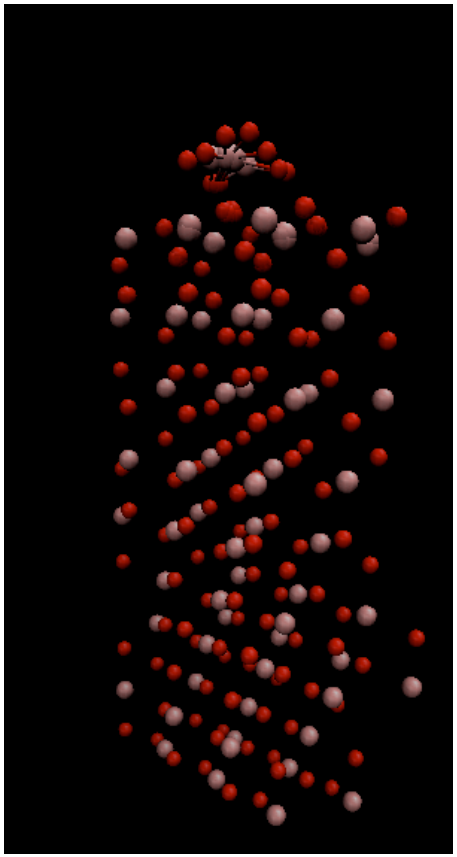

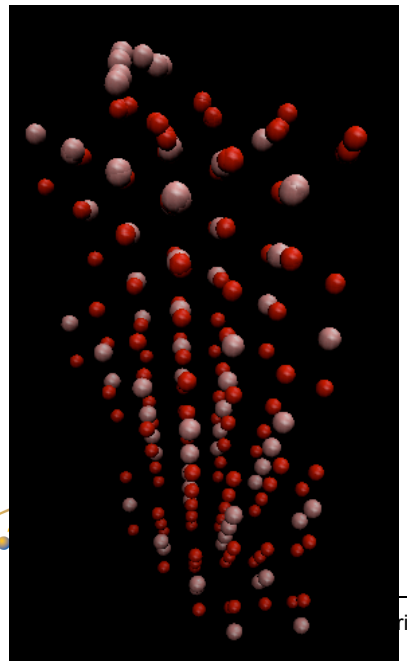

- Difficult to study extended Xe clusters due to size effects.
- Investigate limiting case represented by a (111) surfaces.
- UO_2 species have a barrier of 1.01 eV on (111) surfaces.
- U atoms have a barrier of 1.26 eV on (111) surfaces.
- Sub-surface U vacancies have a barrier that is about 1 eV lower than bulk barriers.
- Simplified model, rate limiting step for bubble diffusion? Contribution to intermediate T gas release?

UO_{2+x} and U_4O_9 structure models

Bevan *et al.*[1] proposed the so-called cubo-octahedron cluster for UO_{2+x} and U_4O_{9-y}.

Cubo-octahedron

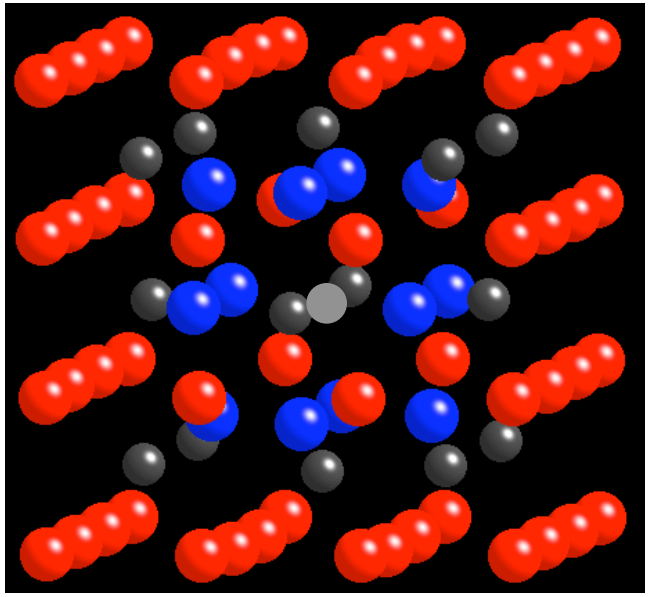

The point defect character in UO_{2+x} was shown to be a function of T and x.

Willis *et al.*[1] found clustering of interstitial-like oxygen ions; introduced to types of interstitial ions, O' and O'', to explain neutron diffraction data.

Willis 2:2:2

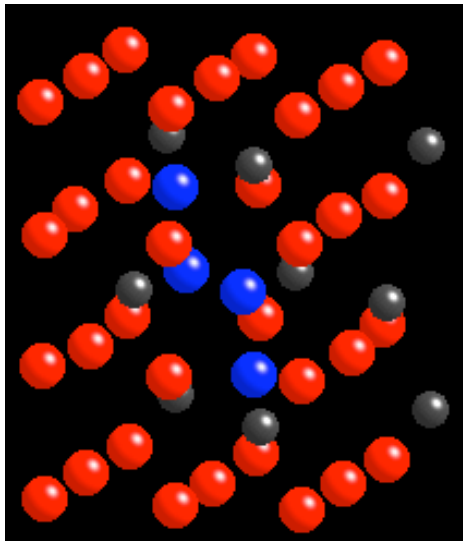

Willis 4:3:2

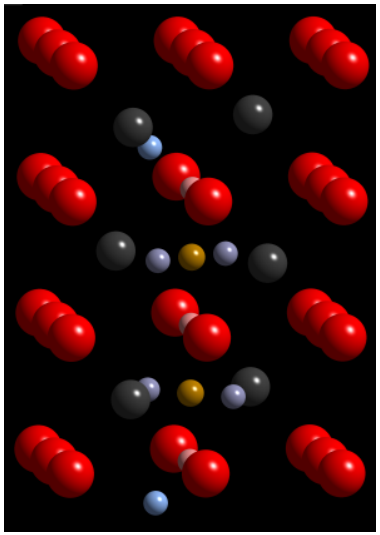

Failed to build U_4O_9 structure model based on the Willis 2:2:2 cluster.

[1] J. Solid State Chem., 61, 1 (1986).

[2] Inorg. Chem. 43, 6922 (2004).

Di-interstitial and quad-interstitial clusters in UO_{2+x} from DFT

- I_2^X is the most stable configuration of di-interstitials, less stable than I_1.
- I_4^X is the most stable state of excess oxygen ions in UO_{2+x}
- Although related, details differ from Willis and cuboctahedral clusters found from neutron diffraction.

Split di-interstitial (I_2^X)

0 eV (r→∞)

$UO_{2.0625}$

+0.16 eV/O ($2I_1$)

+0.19 eV/O (I_2^X)

+0.32 eV/O (I_2^0)

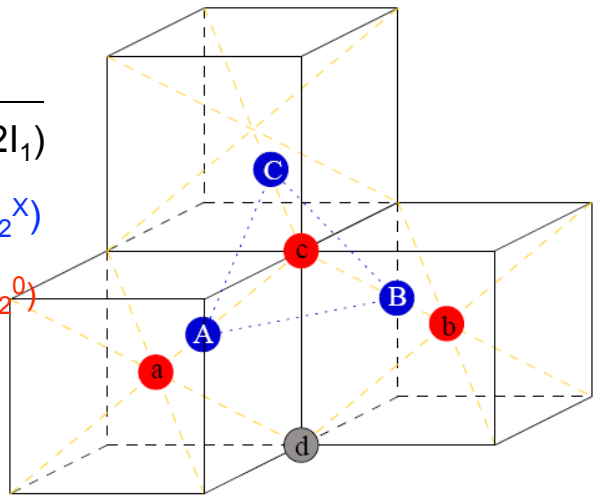

The split di-interstitial (blue) is formed from two NN octahedral interstitials that dislocate a regular oxygen ion (red).

Split quad-interstitial (I_4^X)

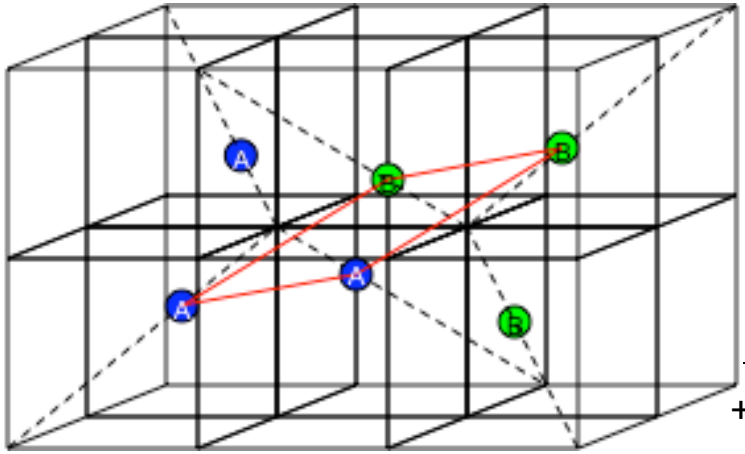

0 eV (r→∞)

$UO_{2.125}$

+0.21 eV/O ($4I_1$)

-0.18 eV/O (I_4)

+0.04 eV/O (I_5)

Two split di-interstitials (blue and green) make up a stable cluster in AnO_{2+x}.

Diffusion of Split Di-interstitials

- Split di-interstitial (I_2^X) can diffuse via intermediate state which is octahedral I_2 structure (I_2^O)
- Migration barrier is 0.47 eV, compared to 0.81 eV for mono-interstitials (interstitialcy mechanism).

Collaboration with C. Deo et al., Georgia Tech.

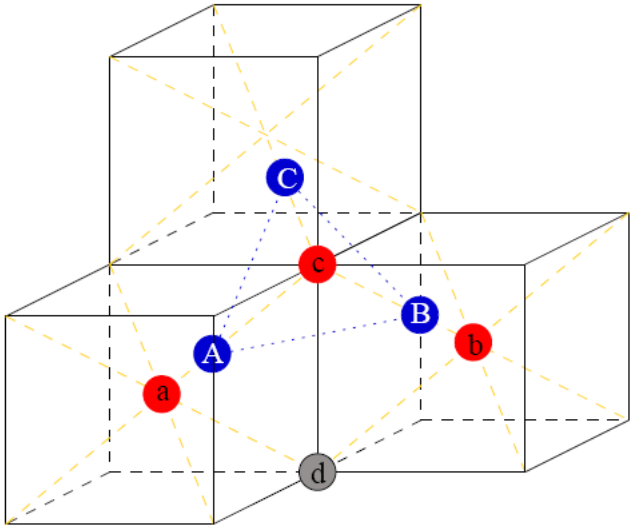

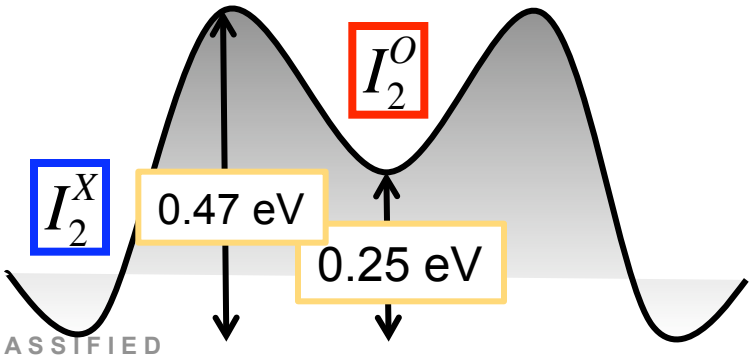

Diffusion of Split Quad-Interstitials

- Split quad-interstitial (I_4^X) can diffuse via one component I_2^X "rotating" to new position
- Migration barrier is 0.97 eV, compared to 0.81 eV for mono-interstitials.

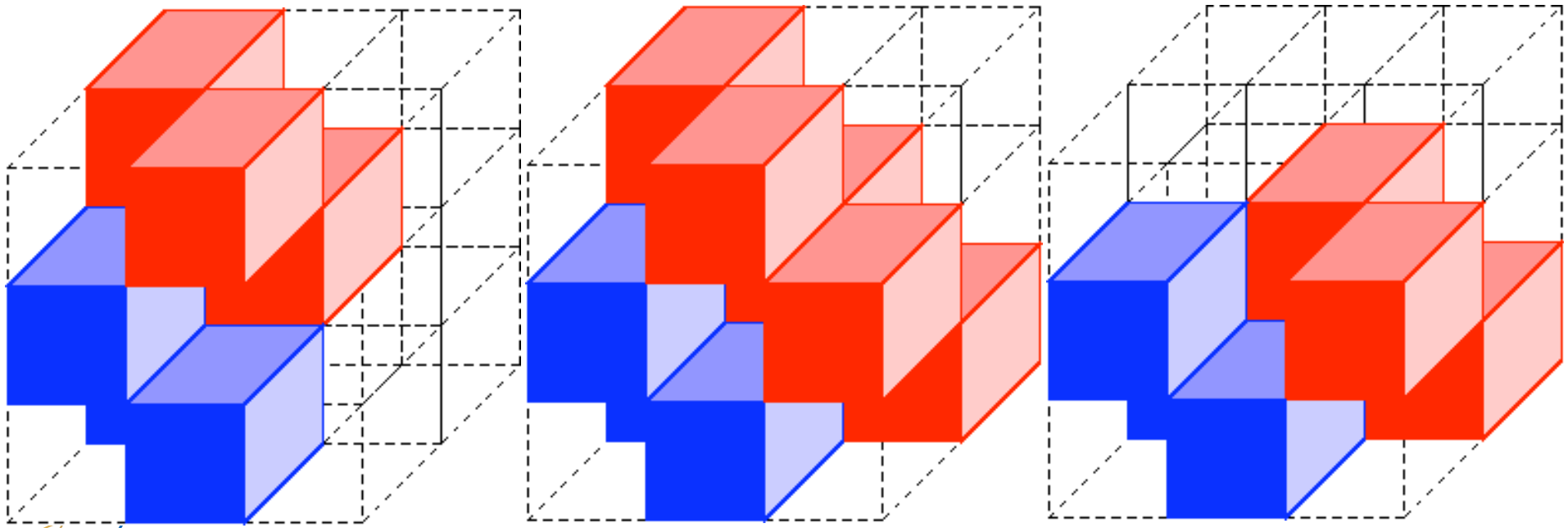

kMC Models for Oxygen Self-Diffusion

Taku Watanabe, Rakesh Behera and Chaitanya Deo

Georgia Institute of Technology

- **Model 1: mono-interstitials only (Murch model)**
  - I_1 diffuse with barrier of 0.81 eV
  - I_1 block all nearest neighbor sites
- **Model 2: mono- plus di-interstitials**
  - Philosophy: as simple an extension of Murch as possible
  - I_1 diffuse with barrier of 0.81 eV
  - I_2 form when 2 I_1 become neighbors
  - I_1 can be neighbors of at most one other I_1 (forming I_2)
    - If an I_1 tries to jump to a site where it would neighbor more than one other I_1, that move is unallowed
  - I_2 diffuse with barrier of 0.47 eV
    - I_2 cannot be nearest neighbor of any other species (like Murch blocking)
  - I_2 are higher in energy than 2*I_1 by 0.38 eV (from LDA+U)
  - Breakup barrier of I_2 would be 0.43 eV (0.81-0.38)
    - Position of new I_1 would depend on available sites

Diffusion: Theory vs Experiment

- KMC simulation of oxygen self-diffusion in UO_{2+x} at 1073 K
- Results agree well at low x
  - Likely describing mono-interstitial diffusion well
- At larger x, I_1 model quickly falls off, in disagreement with experiment
- By including the split di-interstitial mechanism, we are able to better reproduce the experimental data.
  - Mainly due to different different blocking
- Larger clusters for high x? I_1 or I_2 vs. I_4 barriers agree with conductivity experiments.

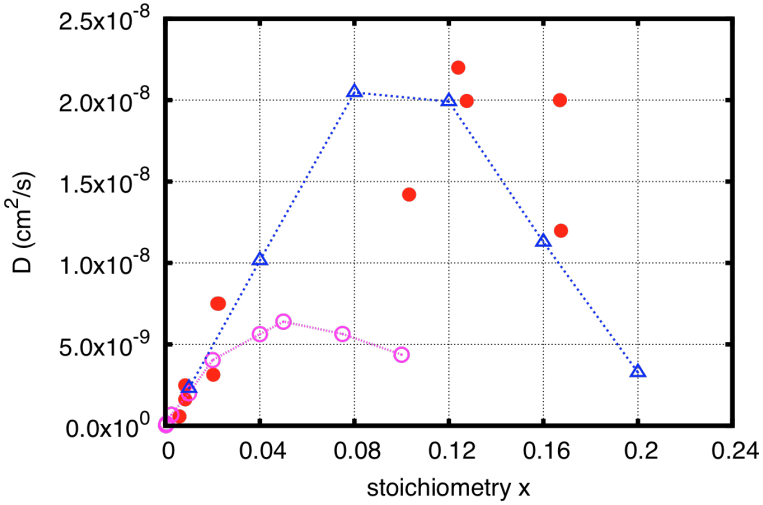

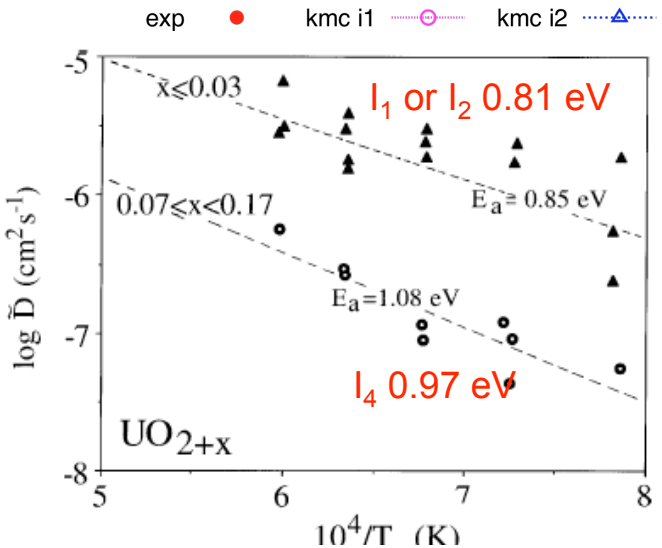

P. Ruello, G. Chirlesan, G. Petot-Ervas, C. Petot, L. Desgranges, Journal of Nuclear Materials **325, 202–209 (2004).**

Improved Description of Cluster Diffusion in UO_{2+x}

Quad-interstitial

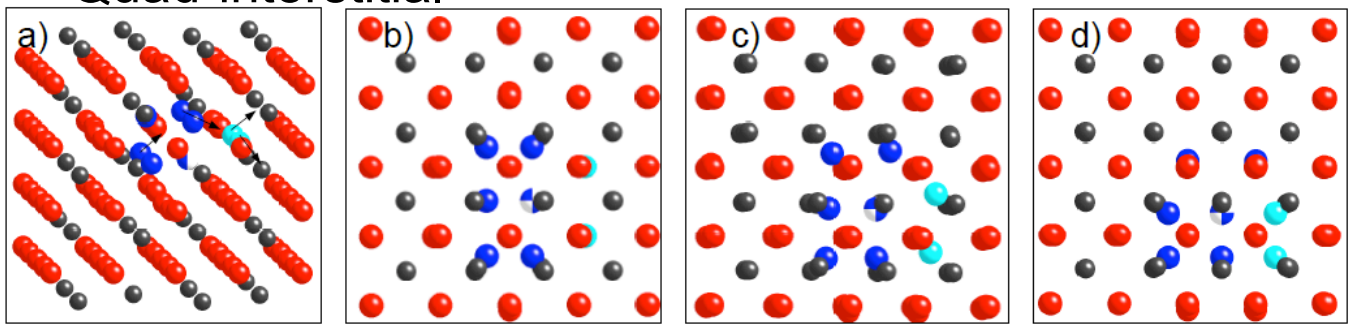

Ruello et al.

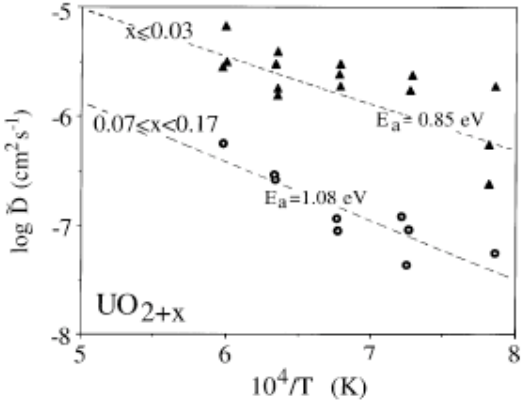

Di-interstitial

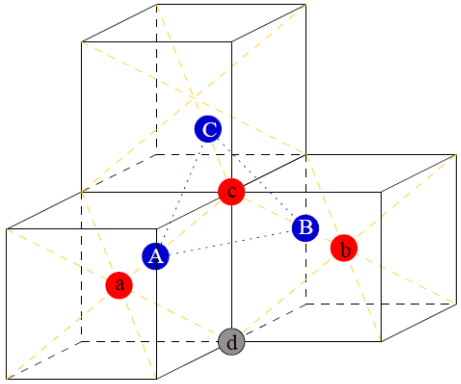

Mono-interstitial (from Dorado et al.)

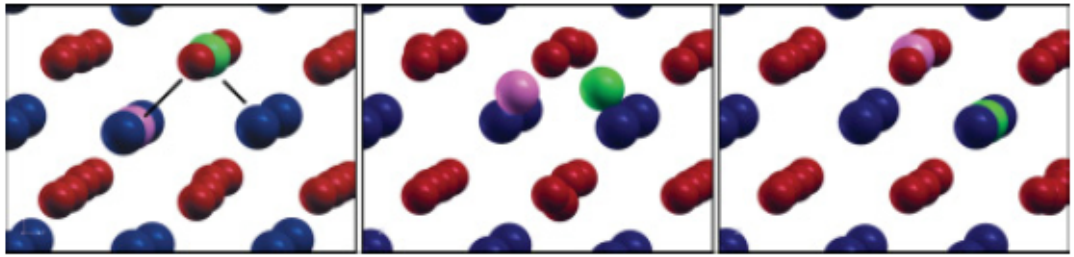

- Exp. barriers: I_1:~1.3 eV, I_2: 0.85 eV, I_4:1.08 eV
- Calculated barriers: I_1:1.31 eV, I_2: 0.87 eV, I_4:1.13 eV
- Implement in kMC for upscaling to continuum.

Conclusions

- DFT to establish that bulk Xe diffusion in $UO_{2\pm x}$ occurs by binding a second V_U to the Xe trap site clusters.
- Accurate activation energies for Xe and U transport from DFT when charge compensation, clustering and thermo-chemistry is accounted for.
- Initial analysis of gas release models with respect to DFT database indicate possible discrepancies for in particular the intermediate temperature regime.
- U (111) surface diffusion was investigated as a model system for diffusion of small fission gas bubbles. An activation energy of 1.0-1.2 eV was predicted for the rate limiting step.
- Oxygen transport as function of stoichiometry (x in UO_{2+x}) studied with a combination of DFT and kMC. Good agreement with experimental measurements when formation of di-interstitial and quad-interstitial clusters are accounted for.